Pharm Res (2015) 32:2625–2635
DOI 10.1007/s11095-015-1648-8

RESEARCH PAPER

Investigation of a Degradant in a Biologics Formulation Buffer Containing L-Histidine

Chunlei Wang • Aaron Yamniuk • Jun Dai • Sike Chen • Paul Stetsko • Noah Ditto • Yingru Zhang

Received: 29 December 2014 / Accepted: 3 February 2015 / Published online: 12 February 2015

ABSTRACT

Purpose An unknown UV 280 nm absorbing peak was observed by SEC for protein stability samples formulated in L-histidine during a stress stability study. Understanding the source would enhance the confidence in the SEC results. We identified the unknown peak, studied the cause, and evaluated ways to eliminate it.

Methods The unknown peak was fractionated by preparative size exclusion chromatography separations, and subsequently analyzed by Hydrophilic Interaction Chromatography (HILIC) coupled with Time-of-Flight (TOF) high resolution mass spectrometry. The possible degradation was also studied with the presence of different excipients, including metal cations, chelating agents, and amino acids.

Results The unknown peak was identified to be *trans*-urocanic acid, a degradant of histidine, based on evidences from HILIC retention time, UV profile, accurate mass measurement, *trans-cis* isomerization, and *pI* measurement. The degradation from histidine to urocanic acids was not affected by the presence of Fe^{2+}, but slightly activated by Mn^{2+}. The chelating agents, EDTA and DTPA, counteracted the Mn^{2+} effects. This degradation was evidenced to be caused by contamination. Adding alanine or cysteine as an excipient was found to reduce this degradation by 97 and 98%, respectively.

Conclusions L-histidine formulation buffer can be contaminated to induce histidine degradation to *trans*-urocanic acid, which shows a large UV 280 nm absorbing peak at the total permeation volume under SEC conditions. Amino acids alanine and cysteine effectively inhibit this histidine degradation.

KEY WORDS degradation · histidine formulation · urocanic acid

ABBREVIATIONS

2-IA	2-imidazolecarboxaldehyde
4-IA	4(5)-imidazolecarboxaldehyde
DTPA	Diethylene triamine pentaactic acid
EDTA	Ethylenediamine teracetic acid
TBHP	*Tert*-butylhydroperoxide

INTRODUCTION

Histidine is one of the most commonly used amino acids in biotherapeutic formulations (1). It has been used as an excipient for several marketed biomolecules including Herceptin® and BeneFIX® (2). In addition to being used as a buffering agent, histidine can physically stabilize biomolecules. Specifically, the beneficial effects observed in histidine formulations include reduced solution aggregation upon freezing and thermal stress (3, 4), inhibition of aggregation growth during lyophilization and subsequent storage (3, 5), preservation of enzymatic activity after spray drying (2), and reduced viscosity of antibody solutions (3). The mechanism of histidine's stabilizing effects during lyophilization has been studied using calorimetry (6) and Raman spectroscopy (7). It was found that

C. Wang (✉) • J. Dai • S. Chen • Y. Zhang
Bioanalytical and Discovery Analytical Sciences, Research & Development, Bristol-Myers Squibb Company, Route 206 and Province Line Road, Princeton, New Jersey 08543, USA
e-mail: chunlei.wang@bms.com

A. Yamniuk • N. Ditto
Department of Discovery Protein Science, Research & Development, Bristol-Myers Squibb Company, Route 206 and Province Line Road, Princeton, New Jersey 08543, USA

P. Stetsko
Discovery Pharmaceutics, Research & Development, Bristol-Myers Squibb Company, Route 206 and Province Line Road, Princeton, New Jersey 08543, USA

histidine interacts with proteins via weak interactions, such as ion-dipole and/or hydrogen-bonding (6), and can protect the antibody against lyophilization induced secondary structure changes (7). In one study (8) when histidine was used as a formulation buffer, however, a significant loss of potency of the monoclonal antibody was observed, which was attributed to a product from histidine oxidation (8, 9). In another study, histidine was reported to undergo photooxidation to produce photosensitizers, which mediate photodegradation of a monoclonal antibody (10).

The oxidation degradation of histidine has been widely reported (10–17). Histidine can be oxidized by the irradiation of light (12, 13) or the presence of hydrogen peroxide and metal cations (14–17), such as the Fenton reaction (14). The photooxidation of histidine is triggered by singlet oxygen attacking its imidazole ring to form an endoperoxide intermediate (13), which undergoes further decomposition to produce a wide variety of end products, including aspartic acid and urea. The imidazole ring is also susceptible to metal catalyzed oxidation to generate mainly 2-oxo-histidine and its ring-opened products, such as aspartate, aspartylurea, and formylasparagine (11, 17). On the other hand, the amino acid functional group can undergo oxidation to produce carbon dioxide, ammonia, aldehydes and carboxylic acids that contain imidazole moiety (14). In the aforementioned study where the potency loss was observed for the antibody formulated in histidine, the histidine oxidation product was identified to be 4(5)-imidazolecarboxaldehyde (4-IA). In another recent publication (18), Amgen scientists observed a "new peak" by size exclusion chromatography (SEC) for samples in histidine buffer. The authors then stressed histidine with *tert*-butylhydroperoxide (TBHP), reasoning that peroxide is likely present in the polysorbate excipient used, and identified several known degradation products when monitoring at UV 260 nm, including 4-IA (18). Interestingly, no analytical data on the "new peak" observed by SEC was presented, nor was its identity confirmed.

During our stress stability tests of biologics in histidine formulations, we also observed an unknown peak with significant UV 280 nm absorbance, which also absorbs at 260 nm, at the total permeation volume under SEC conditions. The appearance of such a peak, although seemingly random, had been observed during several Discovery-stage stressed stability studies at a couple of our Research laboratories. In this study, we perform the analytical work on the protein stability samples in which the extra UV absorbing peak is observed to elucidate the identity of the unknown peak. Furthermore, additional experiments are performed to reproduce this degradation and identify excipients that can suppress it.

MATERIALS AND METHODS

Materials

The histidine used for protein stability studies were FCC and multi-compendial grade, product number 2081 from JT Baker (Center Valley, PA, USA). Another batch of histidine used for comparison in the excipients study was BioUltra grade, product number 53319 from Sigma-Aldrich (St. Louis, MO, USA). Chelating agents ethylenediamine teracetic acid (EDTA), diethylene triamine pentaactic acid (DTPA), Chromasolv gradient grade acetonitrile and formic acid were also from Sigma-Aldrich. Chemicals including glycine, cysteine, and *cis*-urocanic acid standard were from Sigma. Metal salts cadmium chloride, ferrous sulfate hydrate, manganese(II) chloride, oxidizing agent *tert*-butylhydroperoxide (TBHP), and reference standards 4(5)-imidazolecarboxaldehyde (4-IA), 2-imidazolecarboxaldehyde (2-IA), and 4-imidazoleacrylic acid (or *trans*-urocanic acid) were from Aldrich. Alanine was obtained from Fluka. Ammonium acetate was from JT Baker. High-purity water was supplied by the Barnstead Nanopure system from Thermo Scientific (Waltham, MA, USA). The therapeutic proteins used in the study were produced internally at Bristol-Myers Squibb (BMS), with high molecular aggregates at less than 5% level.

Stability Samples

Increasing levels of the UV 280 nm absorbing species were observed in multiple stability studies where histidine was used to formulate different biologics samples, including adnectins, pegylated protein therapeutics, and monoclonal antibodies. In the example shown, a pegylated protein therapeutic was formulated at 7.5 mg/mL using 20 mM histidine and 250 mM sucrose at pH 6.5. The samples were incubated at 25°C for 1 week and 40°C for another 4 weeks.

Isolation of the Unknown Peak

The unknown peak was isolated from multiple injections of the stability sample on an analytical SEC using no salt solvents. Specifically, the isolation was conducted on an Agilent (Santa Clara, CA) 1100 HPLC system with TSKgel G3000SWxl, 300×7.8 mm column (TOSOH Bioscience, King of Prussia, PA) using water/acetonitrile/formic acid 80/20/0.5 as mobile phase solvent running at 1 mL/min. The peak at total permeation volume with 280 nm absorbance was collected, and concentrated by rotary evaporation before additional analysis.

Identification of the Unknown Peak in Stability Samples

The concentrated sample fraction was analyzed by liquid chromatography/mass spectrometry (LC/MS) on an Agilent 6224 TOF MS interfaced to an Agilent 1290 UHPLC. Chromatographic separations were achieved employing a 150× 4.6 mm, 5 μm, ZIC-HILIC column (EMD Millipore, Billerica, MA) with gradient elution at 0.7 mL/min. The column was held at room temperature of about 22°C. Mobile phase A was acetonitrile with 0.1% formic acid, and B was water with 0.1% formic acid. A linear gradient was formed from 10 to 50% mobile phase B in 15 min. A 2 μL injection was used. Positive electrospray ionization (ESI) MS data were acquired from m/z 50 to m/z 1100. The instrument was operated at 20, 000 resolution with an acquisition rate of 1 spectrum/s. Hexakis(2,2,3,3-tetrafluoropropoxy)phosphazine, at m/z 922, was used as internal standard for mass calibration. Additional instrumental settings are as following: capillary voltage 3.5 kV; nebulizer gas 15 psi; drying gas 5 L/min; drying gas temperature 350°C; fragmentor 130 V; skimmer 65 V; OCT 1 RF Vpp 750 V.

The imaged capillary isoelectric focusing (icIEF) was performed on an iCE280 system (ProteinSimple, Santa Clara, CA) using a fluorocarbon coated capillary, 100 μm× 50 mm. Samples were diluted to 0.2 mg/mL using a solution that contains 0.35% methylcellulose, 4% Pharmalyte of pH 3–10, 4 M urea and 1% *pI* markers. The anolyte was 0.1 M phosphoric acid; catholyte 0.1 M sodium hydroxide. The icIEF was achieved by two-step focusing, i.e., 1.5 kV for 4 min and 3.0 kV for 11 min.

Reproducing the Histidine Degradation

Three histidine stock solutions (His-A, His-B and His-C) at 20 mM were prepared. His-A was the original histidine stock solution for our stability studies and was kept in the refrigerator. In one monoclonal antibody stability study, the histidine degradant that gives UV 280 nm absorption was also observed in the control buffer. His-B was composed of 97% His-A and 3% of the degraded histidine control buffer. His-C was prepared at a different lab using a different source of histidine from Sigma-Aldrich. The degradation was only observed in the sample set prepared from the His-B.

To investigate their effects on the observed histidine degradation, different additives were mixed into the 20 mM histidine stock solutions to afford final samples of 16 mM histidine with various excipients. These excipients included 100 mM oxidizing agent TBHP, 0.2 mM ferrous sulfate, 0.2 mM manganese (II) chloride, and 0.2 mM cadmium chloride. In addition, the combination of each of the above excipients with either 0.2 mM EDTA or 0.2 mM DTPA were also prepared. Histidine samples with EDTA or DTPA were also prepared as controls. Three amino acids, i.e., glycine (Gly), alanine (Ala) and cysteine (Cys) at 20 mM were tested as excipients. Three sets of such samples were prepared in a similar fashion from three different histidine stock solutions. All the samples including blank controls were then incubated at 40°C and monitored by HPLC analysis. An additional set of blank control samples, i.e., 16 mM histidine, were kept at 4°C.

Analyzing the Incubated Histidine Samples

The incubation samples were analyzed using the same ZIC-HILIC column on an Agilent 1100 system. The mobile phase was optimized to improve the separation and peak shapes of possible degradation products identified both in the literature and from the current study. Specifically, the mobile phase A was acetonitrile, and B was 20 mM ammonium acetate aqueous solution. The gradient was 10–50% B in 15 min with a flow rate of 0.7 mL/min.

RESULTS

Observation of Degradation by SEC

In our stress stability study to optimize lead selection, SEC was used to monitor the aggregation rate of protein therapeutics formulated in different buffers at elevated temperatures. During the stability study, an unexpected peak with UV absorbance at 280 nm was observed for samples formulated in pH 6.5 histidine buffer. Figure 1 shows selected SEC chromatograms at different time points of the stability study, i.e., T0, 2 and 5 weeks. The peak at the total permeation volume, i.e. around 13 min, increased with time. By the end of the study, after incubation at 25°C for 1 week and 40°C for another 4 weeks, the unknown peak outgrew the protein peaks based on the integrated UV absorbance at 280 nm (Fig. 1c). The appearance of the unknown peak seemed random and did not correlate with the extent of protein aggregation. It could not be attributed to the protein pegylation either. In fact, the same peak had been observed in stability studies of different types of protein constructs, such as monoclonal antibodies and adnectins, and was even detected in the control histidine buffers during one stability study.

Isolation of the Unknown Peak from Protein Stability Samples

The most direct means for determining the molecular weight of the unknown peak would be to use MS compatible solvents for SEC separations with MS detection. However, this attempt was unsuccessful because the new peak coeluted with formulation buffers, which saturated the MS detector. Thus, additional separation of the unknown from the formulation buffers was needed. We first isolated the fractions of the

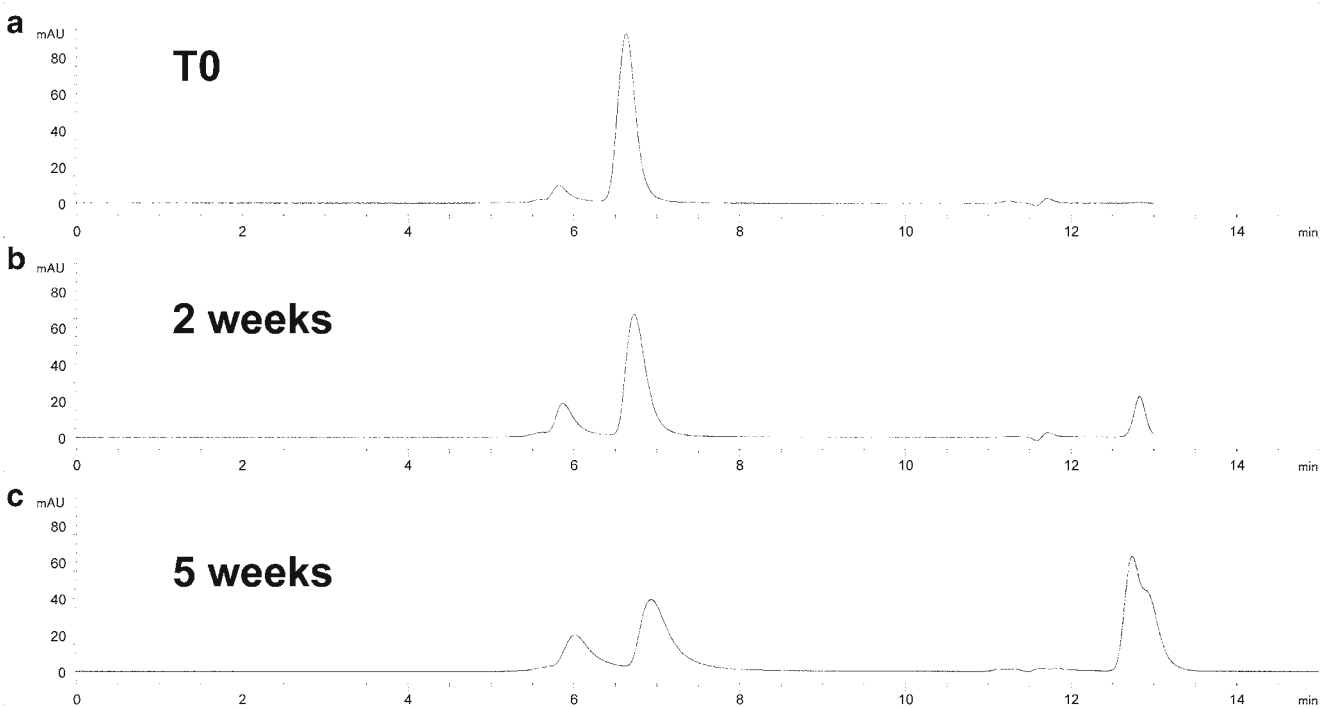

Fig. 1 The SEC chromatograms of a pegylated protein formulated in pH 6.5 histidine buffer at different time points of a stability study: (**a**) beginning of the study; (**b**) 2 weeks; (**c**) 5 weeks. The appearance and growth of the peak at ~13 min was the concern.

growing new peak by preparative SEC. Figure 2 shows the chromatogram of the preparative separation. Instead of using salt buffered SEC solvents, this preparative separation was achieved with water/acetonitrile/formic acid as solvent, in order to avoid introducing extra buffer salts to the fractions. The fractions collected from multiple injections were then combined, and rotoevaporated down to be ready for additional analysis.

Identification of the Unknown Peak

The concentrated fraction from SEC preparative separation was analyzed by LC/MS. Hydrophilic Interaction Chromatography (HILIC) was selected to provide more retention and separation for polar buffer species prior to MS detection. Figure 3a shows the HILIC separation of the SEC fraction peak monitored at UV 280 nm. The peak eluting at 9.4 min corresponds

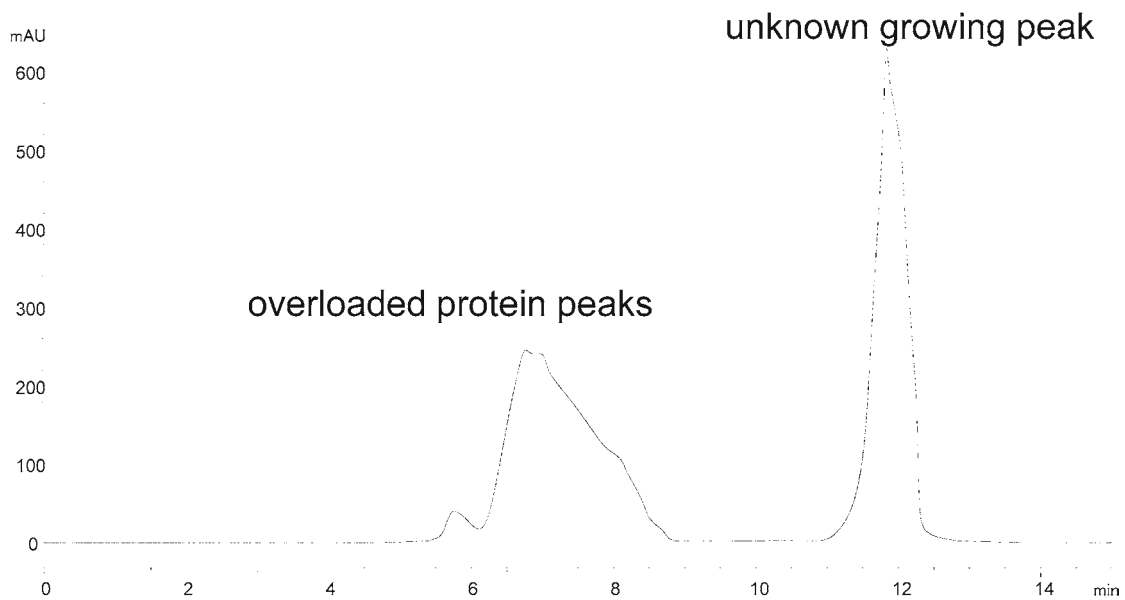

Fig. 2 The preparative SEC chromatogram with 140 μg loading of the protein using water/acetonitrile/formic acid as the mobile phase solvent. The peak at 12 min was collected for further studies.

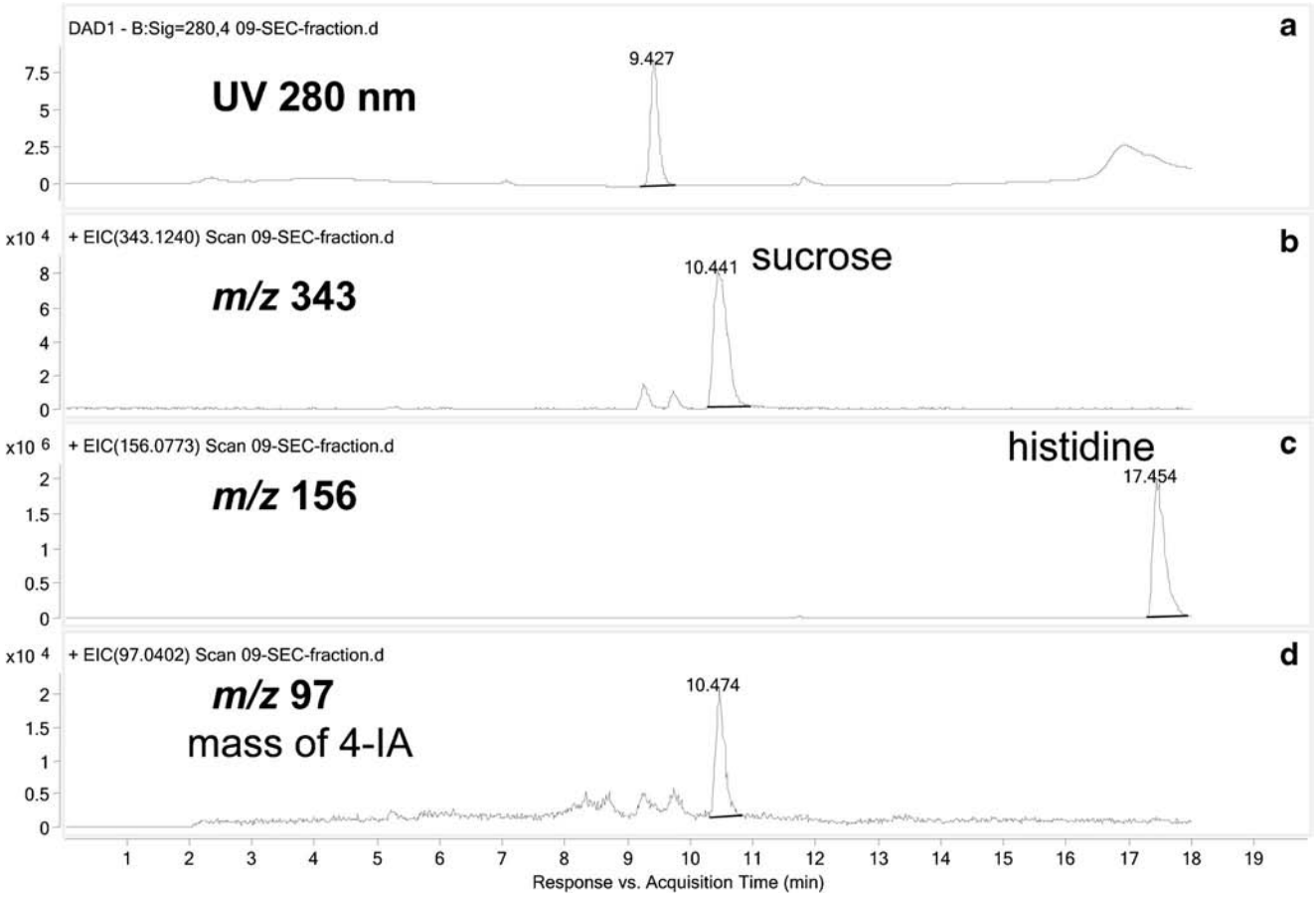

Fig. 3 HILIC chromatograms of the preparative SEC fraction from different detector channels: (**a**) UV 280 nm; (**b**) *m/z* 343 for protonated sucrose; (**c**) *m/z* 156 for protonated histidine; (**d**) *m/z* 97 for protonated 4-IA. The excipients, sucrose and histidine, were separated from the peak of interest. It also confirmed that the unknown peak we observed was not 4-IA, as reported in reference 18.

to the unknown component. The extracted ion chromatograms (EICs) of the excipients sucrose and histidine are shown in Fig. 3b and c, which confirm the separation between the peak of interest and sample matrices under the HILIC condition used. Figure 3d shows the EIC of 4-IA, which was reported by Mason *et al.* to be a possible histidine oxidation product in biologics formulations (18). Comparing Fig. 3a with d, it is clear that the unknown peak that we observed to produce high UV 280 nm absorption is not 4-IA as previously reported. Although there seems to be some 4-IA present in our SEC fractions, its contribution to UV 280 nm absorbance is negligible.

With the additional HILIC separation prior to MS detection, the mass spectrum of the unknown peak is free from the interference of formulation buffer matrices and readily interpretable. The protonated molecule was observed at *m/z* 139, indicating a molecular weight of 138 Da. In source fragmentation produced an ion at *m/z* 94, which was also observed for histidine. This suggests that the degradation product may be histidine related. The nominal mass is 17 Da less than histidine, consistent with loss of ammonia. This was confirmed by accurate mass measurement, *m/z* 139.0508, corresponding to $C_6H_6N_2O_2$, with an error of 4 ppm.

Upon loss of ammonia, histidine forms urocanic acid (19). The injection of the *trans*-urocanic acid standard under the same HILIC condition further confirms this identification. Figure 4 overlays the HILIC chromatograms of the SEC fraction and *trans*-urocanic acid standard. The retention time of the unknown peak in Fig. 4a matches well with the retention time of the *trans*-urocanic acid standard peak in Fig. 4b. The UV profiles of the unknown peak and *trans*-urocanic acid standard match as well. In addition, when the *trans*-urocanic acid was exposed to day light for several days, an additional peak started to appear at 7.1 min, as shown in Fig. 4c. A peak at the same 7.1 min was also observed in the concentrated SEC fraction sample. Instead of being generated directly from histidine, this 7.1 min peak was likely produced from the histidine degradation product (major peak at 9.4 min), when the isolated fraction was exposed to day light. This suggests that the initial degradation product can further change in the same fashion as the *trans*-urocanic acid does. The *trans*-urocanic acid has been reported to partially convert to its *cis*-isomer upon UV irradiation (20). This new peak at 7.1 min had the identical mass as the *trans*-urocanic acid, and was later confirmed to be *cis*-urocanic acid based on the retention time matching with a reference standard.

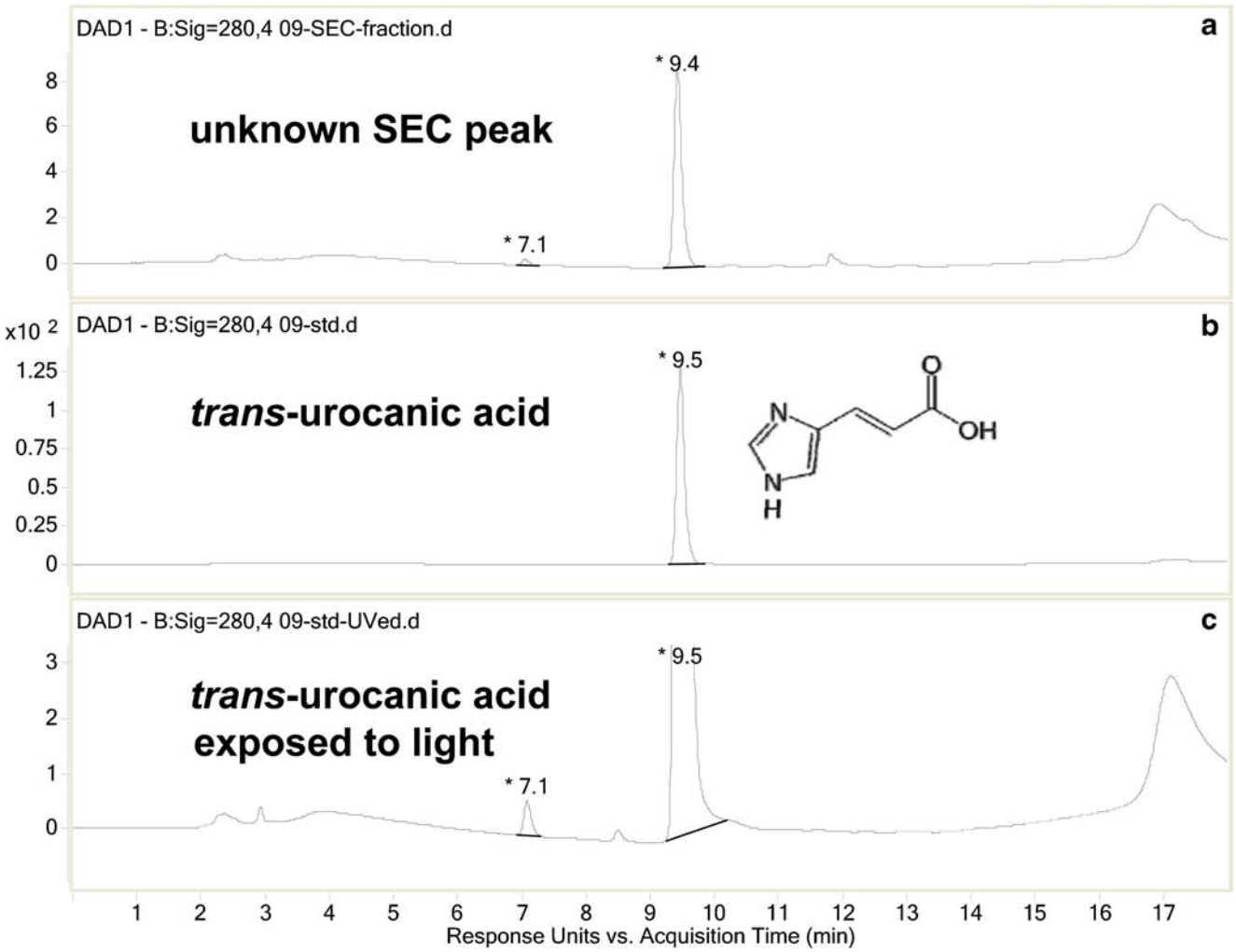

Fig. 4 Overlay of chromatograms under the same HILIC condition: (**a**) SEC fraction of the stability sample; (**b**) *trans*-urocanic acid standard; (**c**) *trans*-urocanic acid standard after exposure to day light for 4 days. The minor peak in A at 7.1 min matches the light induced peak in (**c**), which was later confirmed to be *cis*-urocanic acid.

Finally, the *pI*, as measured by the icIEF, of the unknown and *trans*-urocanic acid are also compared. Figure 5a and b show the icIEF profile of a protein at beginning and end of the study, respectively. The extra peak at a *pI* of around 4.5 in Fig. 5b is attributed to the unknown peak under SEC conditions, which has the identical *pI* as the *trans*-urocanic acid standard (Fig. 5c).

In summary, the unknown peak observed in the stress stability study is determined to be *trans*-urocanic acid, a histidine degradation product, based on the ensemble results of HILIC retention time, UV profile, accurate mass, *trans-cis* isomerization, and *pI* measurement.

Effects of Different Excipients on Histidine Degradation

With the intent to find an excipient that can minimize such degradation, we studied the degradation of histidine in the presence of different additives, including metal cations (Fe^{2+}, Mn^{2+}, and Cd^{2+}), chelating agents (EDTA and DTPA), and amino acids (Gly, Ala and Cys). In addition, we examined the degradation of histidine in the presence of TBHP in order to provide better comparison with the previous histidine degradation study (18). The 16 mM histidine sample incubated with different excipients and their combinations were monitored by HPLC on the same ZIC-HILIC column. The mobile phase was modified to afford separation of *trans*- and *cis*-urocanic acid, as well as 4-IA and 2-IA, which were two possible histidine degradants identified in a previous study (18). The HILIC separation of histidine and its four possible degradation products is shown in Fig. 6. The four histidine related compounds were monitored at UV 280 nm, and histidine was detected at UV 220 nm.

When histidine was incubated with TBHP, we observed the formation of 4-IA, which was consistent with the previous report (18). Both EDTA and DTPA completely inhibited the generation of this oxidation product after 1 week of incubation. Even after incubation at 40°C for 3 months, EDTA and DTPA reduced the formation of 4-IA by 77 and 96%,

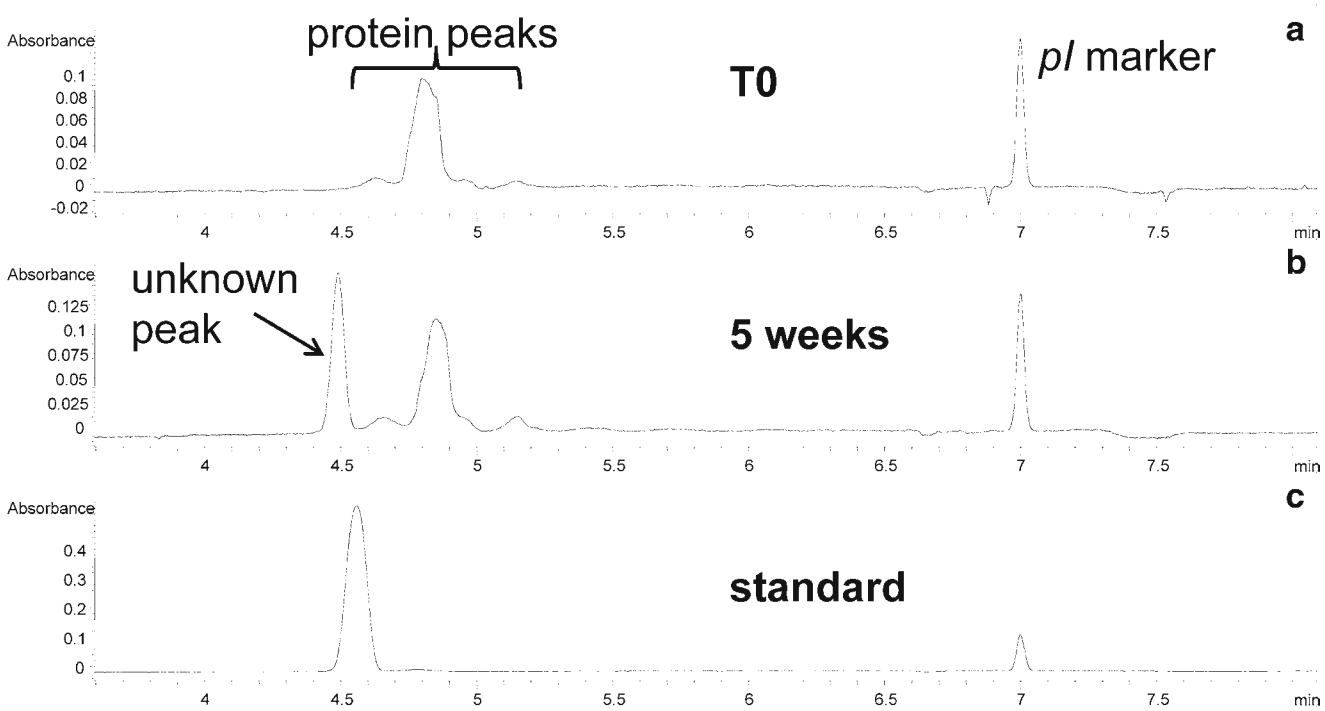

Fig. 5 Overlay of electropherograms from icIEF: (**a**) a protein sample at the beginning of the stability study; (**b**) the protein sample at the end of the stability study; (**c**) *trans*-urocanic acid standard. The *pI* of the extra peak in (**b**) as compared to (**a**) matches the *pI* of the trans-urocanic acid standard.

respectively. This agrees well with the previous study that chelating reagents inhibit growth of 4-IA and that DTPA provides more effective protection than EDTA.

On the other hand, however, when chelating agents are added to histidine and TBPH mixtures, the chromatograms are more complicated with multiple UV 280 nm absorbing

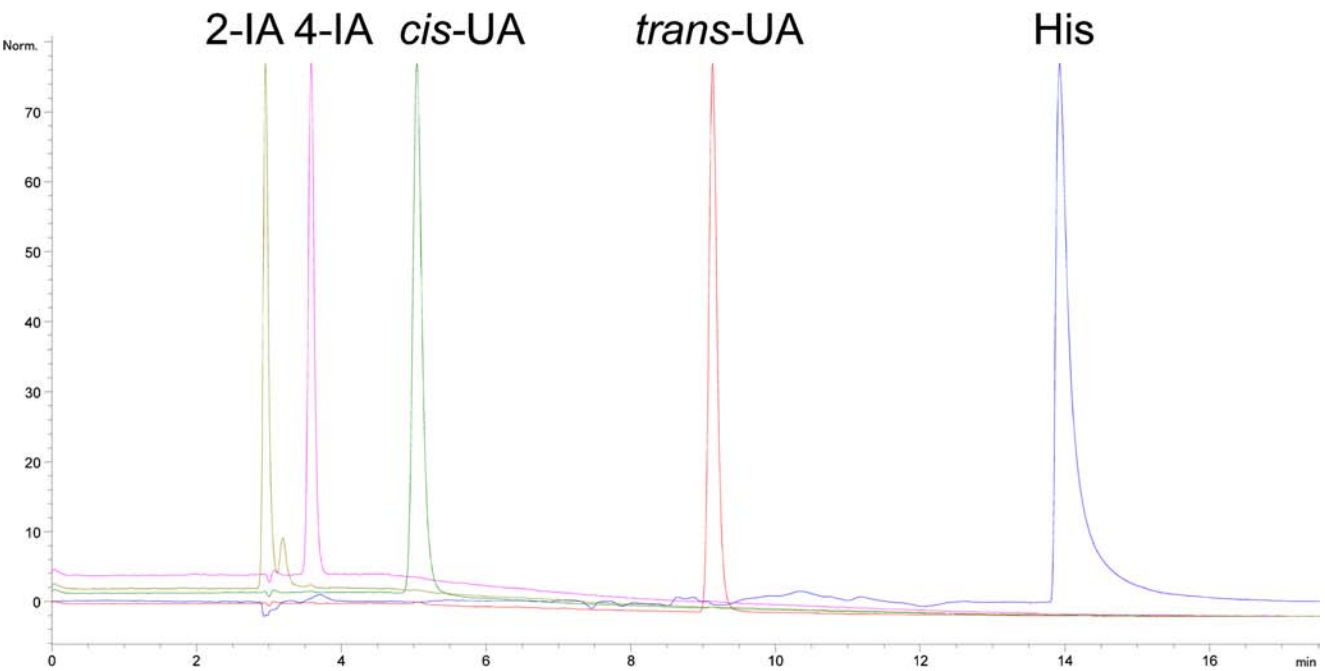

Fig. 6 The separation of histidine and its related compounds under the HILIC condition. From *left* to *right*, the peaks are 2-imidazolecarboxaldehyde (2-IA), 4(5)-imidazolecarboxaldehyde (4-IA), *cis*-urocanic acid (*cis*-UA), *trans*-urocanic acid (*trans*-UA), histidine (HIS). Histidine was detected at UV 220 nm, and others at UV 280 nm.

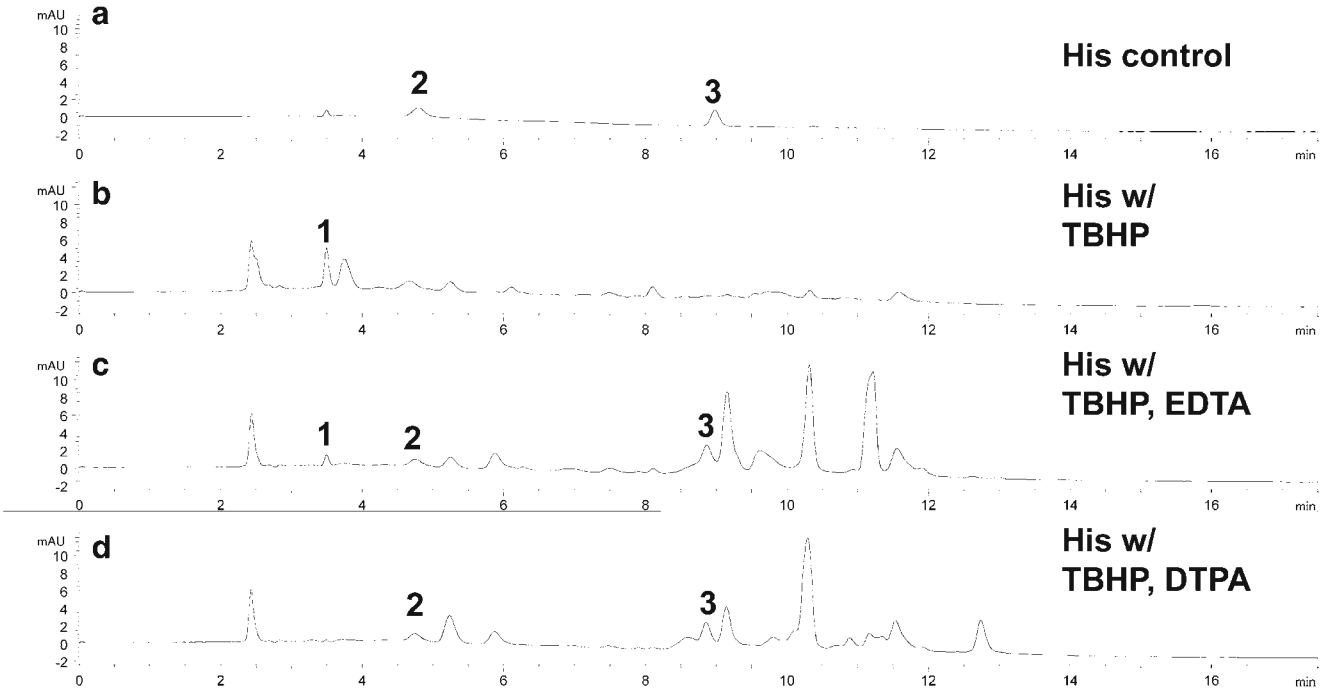

Fig. 7 HILIC chromatograms, plotted in the same scale, of the forced degradation samples of histidine with different excipients: (**a**), control sample, 16 mM histidine; (**b**) histidine with 100 mM TBHP; (**c**) an extra of 0.2 mM EDTA added to (**b**); (**d**), an extra 0.2 mM DTPA added to B. Peak 1 is 4-IA; peak 2, *cis*-urocanic acid; peak 3, *trans*-urocanic acid.

species being generated, as shown in Fig. 7. In addition, the histidine buffer displayed a yellow color at the end of the study when both TBHP and chelating agents were used. The yellow color formation has also been frequently observed for aged histidine buffers (10, 21). It is likely due to oxidation degradation of histidine, although the complete mechanism remains poorly understood. In comparison, the control samples with only TBHP or chelating agents alone remained clear and colorless.

The peak areas of *trans*- and *cis*- urocanic acids produced from histidine with different excipients are listed in Table I. Due to the exposure of the samples to day light, the total peak area of *trans*- and *cis*- urocanic acids are summed and used for discussion. When histidine is oxidized by TBHP to produce 4-IA, no urocanic acids is detected in the sample. However, the histidine oxidation and deamination are less likely to be competing pathways due to the large histidine excess. With the addition of chelating agents, the histidine oxidation to 4-IA is reduced, whereas formation of urocanic acid is increased. It seems that chelating agents not only prevent histidine oxidation, but also stabilized the deaminated product. As a control, the chelating agents alone do not affect histidine degradation to urocanic acids, which also suggests this degradation is not promoted by metals.

Three metals cations, i.e., Fe^{2+}, Mn^{2+}, and Cd^{2+}, were directly tested for their catalytic effects on the histidine to urocanic acids degradation. With the addition of Fe^{2+}, regardless of whether chelating agents were present, the amount of urocanic acids generated are essentially unchanged as compared to the control histidine sample with no additives. On the

Table I The peak area of *cis*- and *trans*- urocanic acid detected at UV 280 nm in forced degradation histidine samples after incubating with different excipients at 40°C for 3 months

Excipients	Peak area of urocanic acid			Relative to Control[a]
	cis-	*trans*-	*cis*+*trans*	
None	12.5	15.9	28.4	100%
TBHP	–[b]	–[b]	–[b]	–
EDTA	11.8	16.5	28.3	100%
DTPA	12.5	16.7	29.2	103%
Fe^{2+}	12.9	16	28.9	102%
Fe^{2+}, EDTA	10.7	18.7	29.4	104%
Fe^{2+}, DTPA	10.2	19	29.2	103%
Mn^{2+}	15.3	19.4	34.7	122%
Mn^{2+}, EDTA	12.5	19.2	31.7	112%
Mn^{2+}, DTPA	16.3	11	27.3	96%
Cd^{2+}	14.6	11.6	26.2	92%
Cd^{2+}, EDTA	10.4	16.3	26.7	94%
Cd^{2+}, DTPA	11.9	15.8	27.7	98%
Gly	10.9	16	26.9	95%
Ala	–[b]	0.9	0.9	3%
Cys	–[b]	0.7	0.7	2%

[a] Calculated using total peak area of *cis*- and *trans*- urocanic acids

[b] not detected

other hand, Mn^{2+} accelerates the generation of urocanic acids by about 20%. The addition of EDTA partially reduces the Mn^{2+} effect, whereas DTPA completely inhibits the Mn^{2+} effect on this degradation. Interestingly, the generation of urocanic acids is reduced by 8% when Cd^{2+} is added.

Finally, the generation of urocanic acids was evaluated in the presence of additional amino acids, including Gly, Ala, and Cys. Figure 8 shows the HILIC chromatograms of histidine samples with different amino acids after incubating at 40°C for 3 months. Comparing Fig. 8a and b, it is clear that Gly has minimal effects on the production of urocanic acids. On the other hand, both Ala and Cys effectively inhibit the degradation of histidine to urocanic acids (Fig. 8c and d). Comparing the chromatograms of Fig. 8c and d, there are some extra peaks with 280 nm absorbance when Cys is used as the additive. Mass spectral data suggests that the major peak in Fig. 8d is cystine, the oxidation product of Cys. In addition, histidine samples containing Cys showed a yellow color at the end of the study. Both the histidine control and the histidine with Ala samples remained clear. In summary, amongst all the excipients tested, Ala proved to be the most effective in preventing histidine degradation to urocanic acids.

It is also worth noting that histidine oxidation is observed even in the histidine control sample with no additives after heat stress at 40°C for 3 months. The peak at 3.5 min in Fig. 8a corresponds to the oxidation product 4-IA. Interestingly, Ala effectively inhibits this histidine oxidation as well (Fig. 8c).

DISCUSSION

Similar to the previous study by Mason *et al.* (18), the current study originated from the observation of a large growing peak with UV 280 nm absorbance under SEC conditions during protein stress stability studies. However, in our case, the investigation (Fig. 1) concluded that the peak with high absorbance at UV 280 nm was *trans*-urocanic acid, instead of 4-IA, the histidine oxidation product identified previously (18). At the end of the 5-week protein stress stability study, approximately 15% of histidine was converted to *trans*-urocanic acid based on mass spectrometry responses. This suggests that the buffering capacity in the formulation is probably still maintained. Unfortunately, the generation of *trans*-urocanic acid was only observed in few protein formulations, and could not be reproduced. This suggested that the histidine converting to *trans*-urocanic acid was caused by an accidental and non-reproducible contamination. However, in the 3 years following our initial analytical work, such histidine degradation occurred several times at a couple of BMS research labs.

During a recent stability study, urocanic acid was detected in the control histidine buffer. This urocanic acid-producing histidine buffer was used as a seed to study the rate of histidine degradation under different excipient conditions. Among three sets of histidine buffers studied, the formation of urocanic acids was only observed in solutions spiked with the urocanic acid-producing histidine solution. In comparison, no urocanic acid growth was observed in the two control sets,

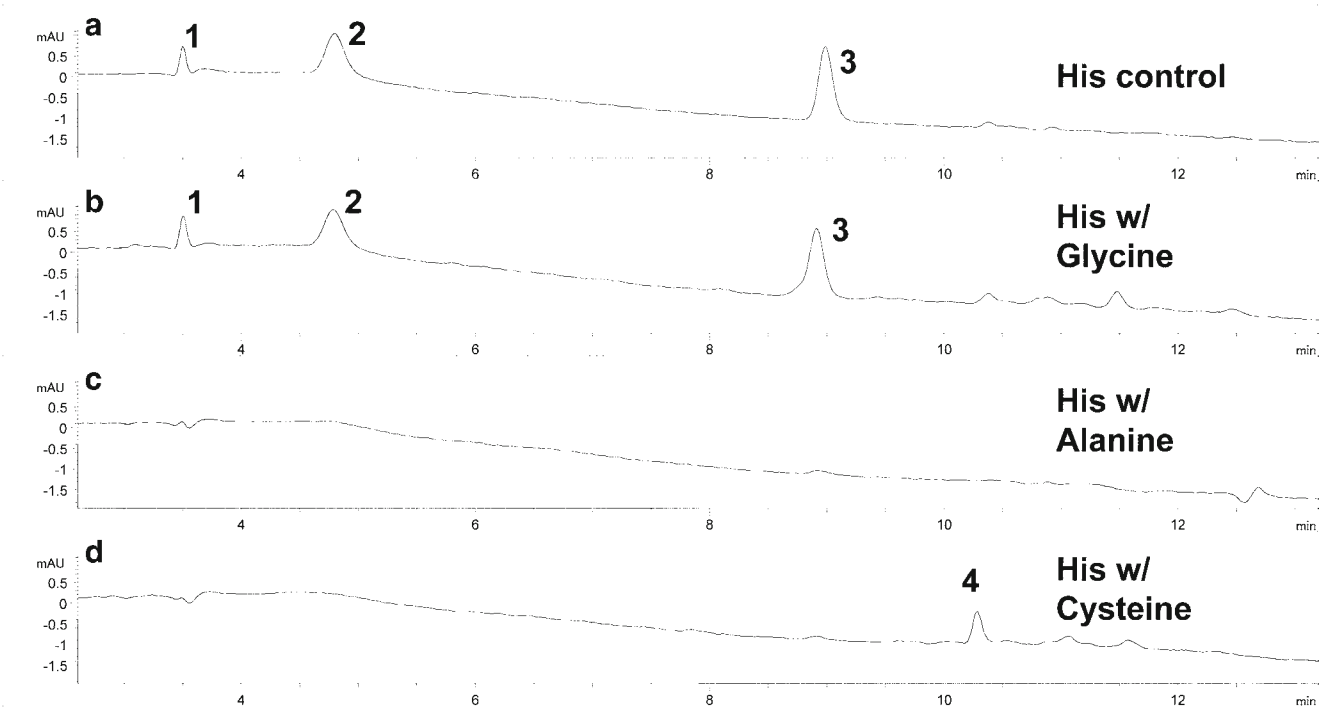

Fig. 8 HILIC chromatograms, plotted in the same scale, of the forced degradation samples of histidine with different excipients: (**a**) control sample, 16 mM histidine; (**b**) histidine with 20 mM Gly; (**c**), histidine with 20 mM Ala; (**d**), histidine with 20 mM Cys. Peak 1 is 4-IA; peak 2, *cis*-urocanic acid; peak 3, *trans*-urocanic acid; peak 4, cystine.

including the original stock solution where urocanic acid growth was observed. This observation confirms that the histidine to urocanic acid degradation cannot be achieved by heat alone, and is caused by contamination during sample preparation steps, instead of from the histidine source material.

The formation of urocanic acid from histidine has been reported in the literature (19, 22–24), but is only known to be catalyzed by mammalian or bacterial histidine ammonia-lyase (HAL). Due to the limited amount of contaminated histidine stock buffer, the effort to isolate and confirm the identity of potential enzymes was not pursued. Instead, we focused on the study of degradation inhibition by evaluating different additives that were known to affect HAL activity. The HAL activity has been reported to be stimulated by metals (23, 24). Interestingly, we observed no acceleration of the reaction by either Fe^{2+} or Cd^{2+} under our experimental conditions. Addition of Mn^{2+} increased the urocanic acid production by only 20%, as compared to the reported at least 50% activation of bacterial HAL even by lower amount of Mn^{2+} than we used (23, 24). In addition, Givot *et al.* studied the inhibition of HAL from *Pseudomonas putida* (23). They found Gly and Cys were potent competitive inhibitors, whereas Ala showed negligible inhibition for the HAL. We incorporated these three amino acids in our experiments. In comparison, Gly, instead of Ala, was the only ineffective inhibitor among these amino acids for the urocanic acid growth. In summary, the effects of excipients on the generation of urocanic acids were quite different from what was reported for HALs.

Urocanic acid has also been shown to undergo futher metabolism and to be a direct precursor of glutamic acid by both bacteria and rats (25, 26). Hence, we also monitored the presence of glutamic acids in the study samples by mass spectrometry. Approximately 4% of urocanic acid was converted to glutamic acid in the protein sample where histidine degradation was observed. On the other hand, less than 1% of glutamic acid was observed in all histidine samples during the study of inhibition on urocanic acid production using different excipients. As a result, except when TBHP is used, urocanic acid content is a useful surrogate for the extend of histidine degradation during our excipient effects study. This is also supported by histidine peak area change at UV 220 nm.

The histidine to urocanic acid degradation we observed is likely also enzymatically catalyzed, because there is no chemical catalyst reported for histidine deamination reaction in literature so far. In addition, the lab where the contamination was suspected has no exposure to complicated organic or inorganic materials. While additional studies are needed to completely understand this degradation, we can infer some characteristics of the culprit enzyme based on the study of exicipients' effects on the urocanic acids generation. Firstly, the enzyme, which is likely originated from microbial contamination, is widely present as evidenced by our observation of urocanic acids at a couple of BMS laboratories in the past 3 years. Secondly, the enzyme activity is temperature and pH dependant. No histidine degradation was observed for sample stored in the fridge or at pH 7. Thirdly, TBHP disrupts histidine deamination reaction likely by either killing contaminating microbes or oxidizing the enzyme to completely lose its enzymatic activity. Interestingly, the HALs have also been reported to lose enzymatic activity upon oxidation, when free thiols form disulfide bonds (23, 24). In comparison, the loss of enzymatic activity after oxidation in our case is less likely to be thiol-related. If thiols were involved in the enzymatic activity, Cd^{2+} would have strongly bound (27) and shown a much greater inhibition effect than was observed experimentally. Finally, the near complete inhibition of urocanic acids production by alanine and cysteine, which are used at a concentration that is similar to histidine, are probably due to their preferential binding to the enzyme. Surprisingly, no deamination product of either alanine or cysteine was observed when extracted ion chromatograms at the appropriate masses were examined.

CONCLUSION

The stability of protein buffer components is an important aspect of formulation development. Buffering agents and their degradants are usually highly polar molecules that are not retained under conventional reversed-phase HPLC conditions. Here, we studied a recurring histidine formulation degradant using HILIC coupled to high resolution MS. The degradation product was identified as a histidine deamination product based on the accurate mass of the parent ion and in source fragmentation. The degradant was further confirmed to be *trans*-urocanic acid based on the HILIC retention time, UV profile, observed *trans-cis* isomerization, and *pI* measurement.

The effects of different excipients on this histidine to urocanic acid degradation were studied. It was found that Fe^{2+} and Cd^{2+} had no effects, whereas Mn^{2+} increased the degradation by 20%. Chelating agents counteracted the Mn^{2+} effects, presumably due to removal of free Mn^{2+}. DPTA was a more effective metal chelator than EDTA, and was able to completely eliminate the additional degradation caused by Mn^{2+}. Amino acids including alanine and cysteine were found to be effective inhibitors of this degradation. Our experimental results suggested that the histidine to urocanic acid degradation is most likely caused by contamination during sample preparation. The different effects of the tested excipients were used to probe the degradation mechanisms. The only currently known pathway for converting histidine to urocanic acid is via an enzymatic reaction with HALs. The response of HAL to different additives is quite different from the excipients effects on the urocanic acids production we

observed here. The complete mechanistic understanding of our observation warrants future investigations.

ACKNOWLEDGMENTS AND DISCLOSURES

The authors would like to thank Dr. Adrienne Tymiak, Bethanne Warrack and Dr. Daniel O'Malley for reviewing the manuscript and providing helpful suggestions.

REFERENCES

1. Kamerzell TJ, Esfandiary R, Joshi SB, Middaugh CR, Volkin DB. Protein–excipient interactions: mechanisms and biophysical characterization applied to protein formulation development. Adv Drug Deliv Rev. 2011;63(13):1118–59.
2. Ajmera A, Scherließ R. Stabilisation of proteins via mixtures of amino acids during spray drying. Int J Pharm. 2014;463(1):98–107.
3. Chen B, Bautista R, Yu K, Zapata G, Mulkerrin M, Chamow S. Influence of histidine on the stability and physical properties of a fully human antibody in aqueous and solid forms. Pharm Res. 2003;20(12):1952–60.
4. Katayama DS, Nayar R, Chou DK, Valente JJ, Cooper J, Henry CS, *et al.* Effect of buffer species on the thermally induced aggregation of interferon-tau. J Pharm Sci. 2006;95(6):1212–26.
5. Österberg T, Fatouros A, Mikaelsson M. Development of a freeze-dried albumin-free formulation of recombinant factor VIII SQ. Pharm Res. 1997;14(7):892–8.
6. Tian F, Sane S, Rytting JH. Calorimetric investigation of protein/amino acid interactions in the solid state. Int J Pharm. 2006;310(1–2):175–86.
7. Sane SU, Wong R, Hsu CC. Raman spectroscopic characterization of drying-induced structural changes in a therapeutic antibody: correlating structural changes with long-term stability. J Pharm Sci. 2004;93(4):1005–18.
8. Subramanian M, Flores-Nate A, Fanget L, Lam V, Kaisheva E. Effect of histidine oxidation on the loss of potency of a humanized monoclonal antibody. AAPS PharmSci. 2001;3(S1):1884.
9. Akers MJ. Excipient–drug interactions in parenteral formulations. J Pharm Sci. 2002;91(11):2283–300.
10. Stroop SD, Conca DM, Lundgard RP, Renz ME, Peabody LM, Leigh SD. J Pharm Sci. 2011;100(12):5142–55.
11. Uchida K. Histidine and lysine as targets of oxidative modification. Amino Acids. 2003;25(3–4):249–57.
12. Tomita M, Irie M, Ukita T. Sensitized photooxidation of histidine and its derivatives. Products and mechanism of the reaction. Biochemistry. 1969;8(12):5149–60.
13. Kang P, Foote CS. Photosensitized oxidation of ^{13}C,^{15} N-labeled imidazole derivatives. J Am Chem Soc. 2002;124(32):9629–38.
14. Dakin HD. The oxidation of amido-acids with the production of substances of biological importance. J Biol Chem. 1906;1(2):171–6.
15. Amici A, Levine RL, Tsai L, Stadtman ER. Conversion of amino acid residues in proteins and amino acid homopolymers to carbonyl derivatives by metal-catalyzed oxidation reactions. J Biol Chem. 1989;264(6):3341–6.
16. Uchida K, Kawakishi S. Identification of oxidized histidine generated at the active site of Cu, Zn-superoxide dismutase exposed to H2O2. Selective generation of 2-oxo-histidine at the histidine 118. J Biol Chem. 1994;269(4):2405–10.
17. Schöneich C. Mechanisms of metal-catalyzed oxidation of histidine to 2-oxo-histidine in peptides and proteins. J Pharm Biomed Anal. 2000;21(6):1093–7.
18. Mason B, McCracken M, Bures E, Kerwin B. Oxidation of free l-histidine by *tert*-butylhydroperoxide. Pharm Res. 2010;27(3):447–56.
19. Raistrick H. On a new type of chemical change produced by bacteria. The conversion of histidine into urocanic acid by bacteria of the coli-typhosus group. Biochem J. 1917;11(1):71–7.
20. Kurogochi Y, Fukui Y, Nakagawa T, Yamamoto I. A note on *cis*-urocanic acid. Jpn J Pharmcol. 1957;6(2):147–52.
21. Lucas K, Maloney K. Methods for inhibiting yellow color formation in a composition. US Patent US20120183531.
22. Mehler AH, Tabor H. Deamination of histidine to form urocanic acid in liver. J Biol Chem. 1953;201(2):775–84.
23. Givot IL, Smith TA, Abeles RH. Studies on the mechanism of action and the structure of the electrophilic center of histidine ammonia lyase. J Biol Chem. 1969;244(23):6341–53.
24. Klee CB. Metal activation of histidine ammonia-lyase: metal ion-sulfhydryl group relationship. J Biol Chem. 1972;247(5):1398–406.
25. Tabor H, Mehler AH, Hayaishi O, White J. Urocanic acid as an intermediate in the enzymatic conversion of histidine to glutamic and formic acid. J Biol Chem. 1952;196(1):121–8.
26. Kraml M, Bouthillier LP. The conversion of urocanic acid to glutamic acid in the intact rat. Can J Biochem Physiol. 1955;33(4):590–8.
27. Xu FF, Imlay JA. Silver(I), mercury(II), cadmium(II), and zinc(II) target exposed enzymic iron-sulfur clusters when they toxify *Escherichia coli*. Appl Environ Microbiol. 2012;78(10):3614–21.